

Research Article

Solid Form of Lipid-Based Self-Nanoemulsifying Drug Delivery Systems for Minimization of Diacerein Adverse Effects: Development and Bioequivalence Evaluation in Albino Rabbits

Mohamed Ahmed Naseef,^{1,2} Howida Kamal Ibrahim,¹ and Samia Abd El-Kader Nour¹

Received 3 May 2018; accepted 27 July 2018; published online 14 August 2018

Abstract. This work aimed to enhance the oral bioavailability of diacerein. The drug was incorporated in self-nanoemulsifying drug delivery system. Ternary phase diagrams were constructed using Capryol™90, Miglyol®812 and isopropyl myristate as oils, Tween®80 and Tween®20 as surfactants and PEG 200 and PEG 300 as co-surfactants. Among a total of 432 formulae, 17 formulae were clear. They were assessed for mean droplet size, polydispersity index (PDI), saturation solubility and transmission electron microscopy. Solid granules were obtained by adsorption on Aeroperl®300. Results for DSC, PXRD, and SEM of prepared granules revealed that diacerein was molecularly dispersed within the formula. Desirability factor was adopted to find the granules with maximum solubility, maximum dissolution efficiency, maximum dissolution rate and percentage of drug dissolved at 5 min and minimum dissolution time and Carr's index. The optimized formula consisted of 10% Miglyol®812, 70% Tween®80 and 20% PEG 200 adsorbed to Aeroperl® 300 with a ratio of 2:1 pre-concentrate:carrier. It recorded a 3.77-fold increase in bioavailability, compared to the marketed product. Such enhancement means lower doses and less gastrointestinal side effects.

KEY WORDS: diacerein; self-nanoemulsifying granules; bioavailability; Aeroperl; dissolution.

INTRODUCTION

Diacerein is a prodrug of rhein used in the treatment of osteoarthritis (1,2). Rhein decreases the incidence of cartilage degeneration and it also stimulates the synthesis of cartilage components (hyaluronic acid, glycosaminoglycan and proteoglycan). This is achieved via inhibition of interleukin-1 synthesis and the release of nitrous oxide (3). The rhein is obtained from metabolism of diacerein in the liver after absorption. The unabsorbed diacerein might be subjected to acid/base hydrolysis in the GIT. This part could stimulate the submucosal neurons resulting in the release of endogenous prostaglandins and acetylcholine in the colon. This mechanism is responsible for the laxative effect of rhein which is the major adverse effect (4). Diacerein has low oral bioavailability (35–56%) which is ascribed to being a Biopharmaceutics Classification System (BCS) class II drug characterized by low solubility and high permeability (5,6). The marketed product has an oral bioavailability ranged from 35 to 56%. Literature showed different trials to improve diacerein bioavailability, such as formulation of nanosuspension and

lipid nanoparticles (1,4), as well as complexation with cyclodextrin (3). Self-nanoemulsifying drug delivery systems (SNEDDS) are employed to enhance the solubility and oral bioavailability of poorly soluble drugs.

Self-nanoemulsifying drug delivery systems are clear isotropic systems containing oils, surfactants and co-surfactants. They form o/w nanoemulsions upon exposure to gastric content and motility (7). Self-nanoemulsifying drug delivery systems show high physical stability upon long-term storage and are suitable for scaling up (8,9). Solid SNEDDS enhance stability and accurate dosing (10). Solid SNEDDS can be formulated via freeze-drying, spray-drying, or by direct adsorption of nanoemulsion pre-concentrates onto carriers (11).

This work aimed to prepare, characterize and optimize diacerein solid SNEDDS. This could enhance both the solubility and oral bioavailability of diacerein with consequent dose reduction.

MATERIALS AND METHODS

Materials

Diacerein powder and diacerein capsule were kindly supplied by EVA, Egypt. Aeroperl®300 was kindly supplied by Degussa, Germany. Capryol™ 90 (propylene glycol monocaprylate, HLB=6) was kindly supplied by Gattefossé, France. Miglyol 812 (caprylic/capric triglyceride, medium-chain

¹Department of Pharmaceutics and Industrial Pharmacy, Faculty of Pharmacy, Cairo University, Kasr El-Eini Street, PO Box 11562, Cairo, Egypt.

²To whom correspondence should be addressed. (e-mail: mohamed.nassef@pharma.cu.edu.eg)

triglycerides, HLB = 15) was kindly gifted by Cermer, Hamburg, Germany. Acetonitrile, rhen and formic acid; Sigma-Aldrich Co., St. Louis, USA. Isopropyl myristate (IPM), PEG 200 and PEG 300 were obtained from Loba Chemie Pvt. Ltd., Mumbai, India. Tween[®]80 (polyoxyethylene sorbitan monooleate, unsaturated C18 fatty acid, HLB = 15), Tween[®]20 (polyoxyethylene sorbitan monolaurate, saturated C12 fatty acid, HLB = 16.7), potassium dihydrogen phosphate and disodium hydrogen phosphate were supplied by El-Nasr Pharmaceutical Chemicals, Egypt. Hydrochlorothiazide was obtained from Genuine Research Center, Cairo, Egypt. Distilled water used was of HPLC grade. All other chemicals were of pure analytical grade.

Construction of Ternary Phase Diagram

Different oils (Capryol[™] 90, Miglyol 812 and IPM), surfactants (Tween[®]20 and Tween[®]80) in addition to PEG 200 and PEG 300 as co-surfactants were used for preparation of 12 different systems. For each system, the 36 possible ratios of the selected surfactant/co-surfactant/oil (S: CoS: O) mixtures ranging from 10 up to 80% for each vehicle were prepared, where the total amount of the three vehicles was always equivalent to 100%. Nine additional co-surfactant-free combinations were prepared in each system at surfactant to oil ratios ranging from 90:10 to 10:90 (12).

Homogenous blends of nanoemulsion preconcentrates were prepared by mixing oils, surfactants and co-surfactants using vortex mixer (Vortex mixer, Julabo Labortechnik, Germany). One gram of each of the prepared nanoemulsion preconcentrates was diluted with 100 mL distilled water with magnetic stirring at 500 rpm for 2 min at room temperature (Wisd Wisestir MSH 20-D, Witeg, Germany). The diluted products were visually examined for clarity against a dark background and were classified as clear, translucent or biphasic. Ternary phase diagrams were plotted for each system using Tri-

plot software Ver.4.1.2 (David Graham and Nicholas Midgley, Loughborough University, Leicestershire, England).

Preparation of Plain Nanoemulsion Preconcentrate Systems

The composition of the prepared 17 formulae is shown in Table I.

Characterization of Nanoemulsion Preconcentrate Systems

Mean Droplet Size and Polydispersity Index

The mean droplet size (MDS) and polydispersity index (PDI) of the formulae showing visual clarity after treatment with distilled water (100-fold) were determined using Zetasizer Nano ZS (Ver.6.20, Malvern Instruments Ltd., Worcestershire, England) using a detector at a scattering angle of 90° to the incident beam at room temperature (13).

Percentage Transmittance

The preconcentrates showing visual clarity were diluted with distilled water (100-fold) and the percentage transmittance of the diluted nanoemulsions were measured at 638.2 nm spectrophotometrically against distilled water as the blank (spectrophotometer UV 1601, PC UV-visible, Shimadzu, Japan) (14).

Self-Emulsification Time

One gram of each of the prepared nanoemulsion preconcentrates was added to 900 mL distilled water in dissolution apparatus II (SR8-PLUS; Hanson Research Corporation, Chatsworth, CA, USA) operated at 50 rpm and temperature

Table I. Compositions and Evaluation of the Formulations Selected from Different Phase Diagrams

Nanoemulsion preconcentrate	Composition			MDS ^a (nm ± SD ^b)	PDI ^c	Self-emulsification time (sec)	Saturation solubility ^d (mg/g ± SD)	Solubility enhancement (Number of folds)
	Oil phase	Surfactant	Co-surfactant					
F1	10% IPM	80% Tween [®] 80	10% PEG 200	22.95 ± 9.98	0.21	43.5 ± 2.6	5.08 ± 0.03	225.6
F2	10% IPM	70% Tween [®] 80	20% PEG 200	44.95 ± 7.14	0.32	50.67 ± 5.2	3.32 ± 0.25	147.64
F3	10% Capryol	80% Tween [®] 80	10% PEG 200	61.81 ± 5.93	0.244	62.11 ± 7.3	4.59 ± 0.16	203.91
F4	10% Capryol	70% Tween [®] 80	20% PEG 200	86.57 ± 4.86	0.272	66.4 ± 4.2	2.27 ± 0.1	100.98
F5	10% Capryol	60% Tween [®] 80	30% PEG 200	182.8 ± 11.46	0.411	70.5 ± 4.72	4.09 ± 0.04	181.56
F6	10% Capryol	80% Tween [®] 80	10% PEG 300	80.96 ± 9.39	0.298	64.9 ± 3.7	3.3 ± 0.28	146.67
F7	10% Capryol	70% Tween [®] 80	20% PEG 300	41.21 ± 4.09	0.203	60.5 ± 4.76	2.17 ± 0.18	96.66
F8	10% Capryol	60% Tween [®] 80	30% PEG 300	170.7 ± 9.33	0.48	68.38 ± 6.7	4.87 ± 0.1	216.49
F9	10% Miglyol	80% Tween [®] 80	10% PEG 200	19.06 ± 1.61	0.346	30.4 ± 3.88	6.25 ± 0.07	277.96
F10	10% Miglyol	70% Tween [®] 80	20% PEG 200	20.46 ± 2.6	0.417	33.6 ± 5.1	6.01 ± 0.06	267.27
F11	10% Miglyol	60% Tween [®] 80	30% PEG 200	24.1 ± 8.62	0.393	35.2 ± 4.7	5.07 ± 0.04	225.27
F12	10% Miglyol	50% Tween [®] 80	40% PEG 200	18.36 ± 2.74	0.26	35.5 ± 4.3	4.51 ± 0.13	200.24
F13	10% Miglyol	40% Tween [®] 80	50% PEG 200	20.1 ± 2.83	0.163	36.2 ± 2.23	3.75 ± 0.08	166.44
F14	10% Miglyol	30% Tween [®] 80	60% PEG 200	36.61 ± 5.07	0.419	40.4 ± 2.4	3.68 ± 0.25	163.33
F15	10% Miglyol	60% Tween [®] 80	30% PEG 300	14.67 ± 1.04	0.2195	34.7 ± 5.1	5.64 ± 0.09	250.53
F16	10% Miglyol	50% Tween [®] 80	40% PEG 300	19.13 ± 1.38	0.287	41.2 ± 4.2	3.62 ± 0.07	160.98
F17	10% Miglyol	40% Tween [®] 80	50% PEG 300	165.73 ± 6.33	0.21	55.2 ± 3.6	4.62 ± 0.06	205.24

^a MDS mean droplet size, ^b SD standard deviation, ^c PDI polydispersity index, ^d saturation solubility of diacerein in water = 22.5 ± 3.22 µg/mL

37 °C. The time for complete emulsification was visually observed (15,16).

Saturation Solubility

Known excess quantity of diacerein was mixed with one gram of each of the selected pre-concentrates in a capped glass vial. They were mechanically shaken in oscillating thermostatically controlled water bath shaker (Julabo SW-20 C, USA) at 50 rpm for 1 day at room temperature. The resulting dispersion passed through a Millipore membrane filter (0.45 μm) for clarification. Then, 100 mL distilled water was added under magnetic stirring at 500 rpm and room temperature for 2 min. The concentration of diacerein was measured spectrophotometrically at λ_{max} 258 nm with reference to a pre-constructed calibration curve at the same wavelength ($r^2 = 0.999$, $n = 3$).

Transmission Electron Microscopy

From the selected formulae with low MDS and PDI and high saturation solubility, F10 was used as an example for investigation via TEM (Jeol JEM 1230, Tokyo, Japan). The morphological examination of the nanoemulsion was performed after treatment with distilled water (100-fold). A drop of sample was added to a collodion-coated 300-mesh copper grid, and after 10 min, the excess dispersion that did not adhere to the collodion was removed with filter paper, then it was stained with one drop of 2% phosphotungstic acid solution for 1 min. After that, the excess was drawn off and the sample was allowed to dry in air and inspected with a transmission electron microscope (17).

Preparation of Solid Nanoemulsion Preconcentrate Granules

Fifty milligrams of diacerein was dissolved in each of the selected nanoemulsion pre-concentrates under magnetic stirrer. After one day of equilibration of the drug loaded formulae, the formulae were adsorbed on AeroPerl powder. This was performed by direct trituration in a glass mortar at 2:1 pre-concentrate: adsorbent ratio. The composition of the developed solid nanoemulsion preconcentrate granules (SNEG) is given in Table II.

Characterization of the Prepared SNEG

Differential Scanning Calorimetry

Five-milligram samples of each of the prepared granules formulae (SNEG 1–5) were heated in hermetically sealed aluminium pan over a temperature range from 25 to 300 °C at a scanning rate of 10 °C/min under nitrogen atmosphere using a differential scanning calorimeter (Mettler-Toledo International Inc., Columbus, OH, USA). The thermogram of the prepared formula was investigated against that of diacerein, and free carrier.

Fourier Transform Infrared Spectroscopy

The prepared granule formulae (SNEG 1–5), as well as the drug and carrier, were recorded using IR spectrophotometer

(Mattson FTIR spectrometer, USA). The IR spectrum was employed to show the similarity and the differences of the solid phase of the prepared SNEG to those of diacerein and AeroPerl 300. One milligram of sample was blended with 200 mg KBr to prepare the KBr disc. The FTIR range started from 4000 to 450 cm^{-1} .

Powder X-ray Diffraction

Diacerein, AeroPerl 300 and the optimized SNEG3 formula were characterized using powder x-ray diffraction (MD-10 mini diffractometer, MTI Corporation, Richmond, CA, USA) under the following conditions: Cu K2 α rays ($\lambda = 1.54056 \text{ \AA}$) and a current of 30 mA with a voltage of 25 kV at a scan rate of 8 deg./min and, in a flat plate $\theta/2\theta$ geometry.

Scanning Electron Microscopy

Diacerein, AeroPerl 300 and the optimized SNEG3 surface characteristics were examined using a scanning electron microscope (JXA-840; JEOL, Tokyo, Japan). Each sample was mounted on a brass stub and then the samples were coated with gold under reduced pressure for 30 s to be electrically conductive. The Photomicrographs were recorded at 20 kv excitation voltage.

Carr's Index

The tapping method was utilized to determine Carr's index for investigation of the flowability of the prepared SNEGs.

Drug Content

The prepared SNEGs were examined for percentage of drug released. One gram of the SNEG was treated with 100 mL of distilled water and blended for 2 min at room temperature, followed by filtration of the resulting dispersion of diacerein using a 0.45- μm Millipore membrane filter. The percentage released of diacerein was measured at 258 nm spectrophotometrically.

The results were subjected to a two-sided one-sample statistical *t* test for comparison between the average drug content and its hypothetical value. All measurements were run in triplicate.

In Vitro Dissolution Study

The study was carried out in triplicate for the prepared SNEG formulae, diacerein powder and the marketed product, each containing 50 mg diacerein, using dissolution apparatus II (SR8-PLUS; Hanson Research Corporation, Chatsworth, CA, USA). The dissolution medium was 900 mL pH 6.8 phosphate buffer, the paddle speed was 50 rpm, and the temperature was kept at $37 \pm 0.5^\circ\text{C}$ (1,2,5,18). At different time intervals of 2, 5, 10, 15, 30, 45 and 60 min, aliquots of 5 ml were collected and replenished with the same volume of pH 6.8 phosphate buffer. Samples were immediately passed through a 0.45- μm Millipore membrane filter and assessed for the concentration of diacerein spectrophotometrically at 258 nm.

Table II. Composition of the Prepared SNEG and Their Evaluations

Formula code	Composition of SNEG			Carr's index (%)	Percentage drug content (%)	DE ₍₀₋₃₀₎ ^a (%)	Q ₅ ^b (%)	DR ₅ ^c (min ⁻¹)	MDT ^d (min)
	Preconcentrate	Carrier	Preconcentrate: carrier ratio						
SNEG1	10% IPM, 80% Tween 80, 10% PEG 200	Aeroperl	2:1	31.52 ± 3.32	100.18 ± 0.25	91.02	75.91	15.18	1.91
SNEG2	10% Miglyol, 80% Tween 80, 10% PEG 200			14.84 ± 1.19	99.25 ± 0.36	93.06	79.14	15.82	1.54
SNEG3	10% Miglyol, 70% Tween 80, 20% PEG 200			23.32 ± 3.88	103.89 ± 4.08	93.16	83.89	16.78	1.66
SNEG4	10% Miglyol, 60% Tween 80, 30% PEG 200			30.65 ± 6.14	100.36 ± 1.07	93.24	82.33	16.46	1.58
SNEG5	10% Miglyol, 60% Tween 80, 30% PEG 300			30.01 ± 3.88	100.59 ± 0.19	92.97	80.1	16.02	1.54

^a DE₍₀₋₃₀₎ dissolution efficiency till 30 min, ^b Q₅ percentage of drug released at time 5 min, ^c DR₅ dissolution rate during first 5 min of dissolution,

^d MDT mean dissolution time

Dissolution efficiency₍₀₋₃₀₎ of marketed product = 28.69 ± 3.73%, Q₅ = 2.14 ± 0.12%, DR₅ = 0.43 ± 0.02 min⁻¹ and MDT = 6.2 ± 0.72 min

Dissolution efficiency₍₀₋₃₀₎ of diacerein powder = 41.06 ± 3.27%, Q₅ = 15.15 ± 7.28%, DR₅ = 3.03 ± 1.45 min⁻¹ and MDT = 4.1 ± 0.1 min

Dissolution efficiency till 30 min (D.E.₍₀₋₃₀₎) was computed according to the following equation (19):

$$D.E. = \frac{\int_0^t y \times dt}{y_{100} \times t} \times 100\% \quad (1)$$

where y is the percentage of dissolved drug at time t .

Mean dissolution time (MDT), percentage of drug released at 5 min (Q₅) and dissolution rate during first 5 min of dissolution (DR₅) were calculated for each tested formula. Mean dissolution time was calculated as follows (20):

$$MDT = \frac{\sum_{i=1}^n t_{mid} \times \Delta M}{\sum_{i=1}^n \Delta M} \quad (2)$$

Optimization of the Prepared SNEGs

A desirability function was adopted for the optimization of the prepared SNEGs according to Derringer and Suich (21). The targeted formula should have the highest Q₅, D.E.₍₀₋₃₀₎, DR₅ and saturation solubility and the lowest MDT and Carr's index.

The equations used for the desirability function of the maximized responses (Q₅, D.E.₍₀₋₃₀₎, DR₅ and saturation solubility in water) are:

$$d1, d2, d3 \text{ or } d4 = \frac{Y_i - Y_{min}}{Y_{target} - Y_{min}} \text{ for } Y_i < Y_{target} \quad (3)$$

$$d1, d2, d3 \text{ or } d4 = 1 \text{ for } Y_i > Y_{target}$$

The equations used for the desirability function of the minimized responses (MDT and Carr's index) are:

$$d5 \text{ or } d6 = \frac{Y_{max} - Y_i}{Y_{max} - Y_{target}} \text{ for } Y_i > Y_{target} \quad d5 \text{ or } d6 = 1 \text{ for } Y_i < Y_{target} \quad (4)$$

Equation for the overall desirability values is the following equation:

$$D = (d1 \ d2 \ d3 \ d4 \ d5 \ d6)^{1/6} \quad (5)$$

where d1–6 are the individual desirability factors for each response and Y_i is the study result.

In Vivo Evaluation

The experiment was performed to determine the pharmacokinetics parameters of diacerein and its absorption from different formulae. The experiment protocol was accepted by the Research Ethics Committee of Faculty of Pharmacy, Cairo University, Cairo, Egypt (PI 911). The test was carried out for two formulae, namely diacerein capsule-EVA pharma (innovative market product) and the optimized formula SNEG3. Six healthy male albino rabbits (2–2.2 kg) were assigned randomly into two groups, three rabbits in each group. Before the start of the study, the rabbits were fasted for 10 h while water was allowed. Each rabbit was administered orally a single dose of one of the prepared diacerein formulae, each containing 9.25 mg of diacerein, in a crossover design with a 2-week washout period (22). Blood samples were removed from the rabbits' marginal ear vein, 1.5 ml each, just prior to drug administration and at a predetermined time intervals of 10, 20, 30, 45, 60, 120, 240, 480 and 720 min after drug administration. The blood samples were stored in heparinized tubes to guard against coagulation of blood till centrifugation for 15 min at 4000 rpm. Finally, the collected clear plasma was deep frozen in capped plastic tubes at –20 °C pending for extraction and analysis.

The analysis involved using a liquid chromatography–tandem mass spectrometry (LC-MS/MS) technique for determination of rhein (the active metabolite of diacerein) concentrations in plasma (1). Chromatographic separations were operated using isocratic mobile phase of 0.1% formic acid in water and acetonitrile (20:80% V/V), and the flow rate was adjusted to be 1 mL/min. The internal standard (IS) was hydrochlorothiazide

(HCZ) solution in acetonitrile (1 $\mu\text{g/mL}$). All frozen plasma samples were allowed to thaw at room temperature. A half milliliter of each plasma sample was mixed with 100 μL of IS in 5-mL glass tubes, and the mixture was subjected to vortexing for 2 min. After that, the samples were treated with 1 mL acetonitrile and vortexed for 2 min followed by 10 min centrifugation at 4000 rpm. Collection of the upper organic phase in the autosampler vials was conducted, followed by injection of 15 μL aliquot into the LC-MS/MS system (Shimadzu prominence series LC, Shimadzu, Japan) equipped with degasser (DGU-20A3), solvent delivery unit (LC-20AB) and auto sampler (SIL-20 AC) that could inject samples on a Luna C₁₈ column (Sunfire, Waters, USA) 50 \times 4.6 mm, 5- μm particle size. The Guard column was phenomenex C₁₈ 5 \times 4.0 mm, 5- μm particle size.

Quantitation was performed using a MDS Sciex API-3200 mass spectrometer (Foster City, CA, USA), equipped with a Turbo™ ion spray interface at 450°C in the negative ion mode. The ion spray voltage was adjusted at -4400 V. Measurement of the ions was carried out in the mode of multiple reaction monitoring, monitoring the transition of the m/z 295.9 precursor ion to the m/z 78.0 for IS and m/z 282.86 precursor ion to the m/z 238.9 for rhein. Quadrupoles Q1 and Q3 were set on unit resolution. The analytical data processing was carried out using Analyst® Software Version 1.6 (Applied Biosystems product line of Thermo Fisher Scientific). All analysis was carried out at ambient temperature.

The rhein plasma concentration-time data was subjected for analysis via Kinetica software version 4.4.1 (Thermo Fisher Scientific Inc.) in order to compute the following pharmacokinetic parameters, the area under the plasma concentration-time curve from time zero to infinity ($\text{AUC}_{0-\infty}$), maximum plasma concentrations (C_{max}), the time of their occurrence (T_{max}), the terminal elimination rate constant and the half-life ($T_{1/2}$) using non-compartmental pharmacokinetic models and the results were statistically analyzed at $p=0.05$.

In Vitro/In Vivo Correlation

Multiple level C *in vitro/in vivo* correlation (IVIVC) was selected to investigate the correlation between the *in vitro* dissolution and *in vivo* diacerein bioavailability for both SNEG3 and the marketed product used. The cumulative percentages diacerein dissolved (10, 30 and 45 min) were correlated with the partial AUCs (AUC_{0-10} , AUC_{0-30} and AUC_{0-45}), calculated using the linear trapezoidal rule. The cumulative percentage diacerein dissolved was set to be the independent variable (X) and the partial AUC was the dependent (Y) variable.

Linear regression analysis was conducted to calculate the coefficient of determination (r^2) using Microsoft Excel 2010 (Microsoft corporation, Washington, DC) (23,24).

RESULTS

Construction of Ternary Phase Diagram

Only five of the prepared 12 systems revealed visual clarity after a 100-fold dilution with distilled water, namely systems I, III, IV, V and VI. Ternary phase diagrams for the five systems showed clear, translucent and biphasic

combinations after dilution with distilled water as in Fig. 1. The shaded area represents the nanoemulsion region (clear and translucent combinations) where the other points represent biphasic combinations. The clear combinations were selected for characterization and formulation because they were expected to have higher transmittance, lower mean droplet size and better self-emulsification properties.

The results revealed that 17 nanoemulsions were obtained out of 432 combinations tried (12 systems \times 36 ratios). The succeeded formulae were based on Tween 80 as the surfactant rather than Tween 20.

In the present study, IPM, Capryol 90 and Miglyol 812 succeeded as oil phases in a ratio of 10% for nanoemulsion formation. Our results also demonstrated that medium-chain-length fatty acids (Miglyol and capryol) had bigger nanoemulsion areas in phase diagrams compared to long-chain fatty acid (IPM). The ternary phase diagrams revealed that co-surfactant-free combinations failed to obtain nanoemulsions in all systems.

Characterization of Nanoemulsion Preconcentrate System

Mean Droplet Size and Polydispersity Index

Table I shows that MDS of the 17 formulae ranged from 14.67 ± 1.04 to 182.8 ± 11.46 nm. Most of the formulations (F1, F2, F3, F4, F6, F7, F9, F10, F11, F12, F13, F14, F15 and F16) had MDS less than 100 nm which indicated nanoemulsion formation. The obtained PDI results varied from 0.16 to 0.48 revealing the nanoemulsion homogeneity.

Percentage Transmittance

The % transmittance of all formulae after a 100-fold dilution ranged from $95 \pm 0.34\%$ to $98.7 \pm 0.55\%$.

Self-Emulsification Time

The self-emulsification times of the prepared formulae are listed in Table I and ranged from 30.4 ± 3.88 to 70.5 ± 4.72 s.

Solubility Determination

The results for saturation solubility of the drug within the prepared nanoemulsion preconcentrates are shown in Table I. Higher drug solubilities were observed in Miglyol-based nanoemulsions (F9 and F10) compared to other oils. Moreover, increasing surfactant (Tween 80) concentration would increase diacerein solubility in the prepared nanoemulsions.

Transmission Electron Microscopy

Transmission electron microscopy for diluted formula F10 showed regular well-identified spherical shape globules with uniform distribution which were correlated with the droplet size obtained by Zetasizer (Fig. 2).

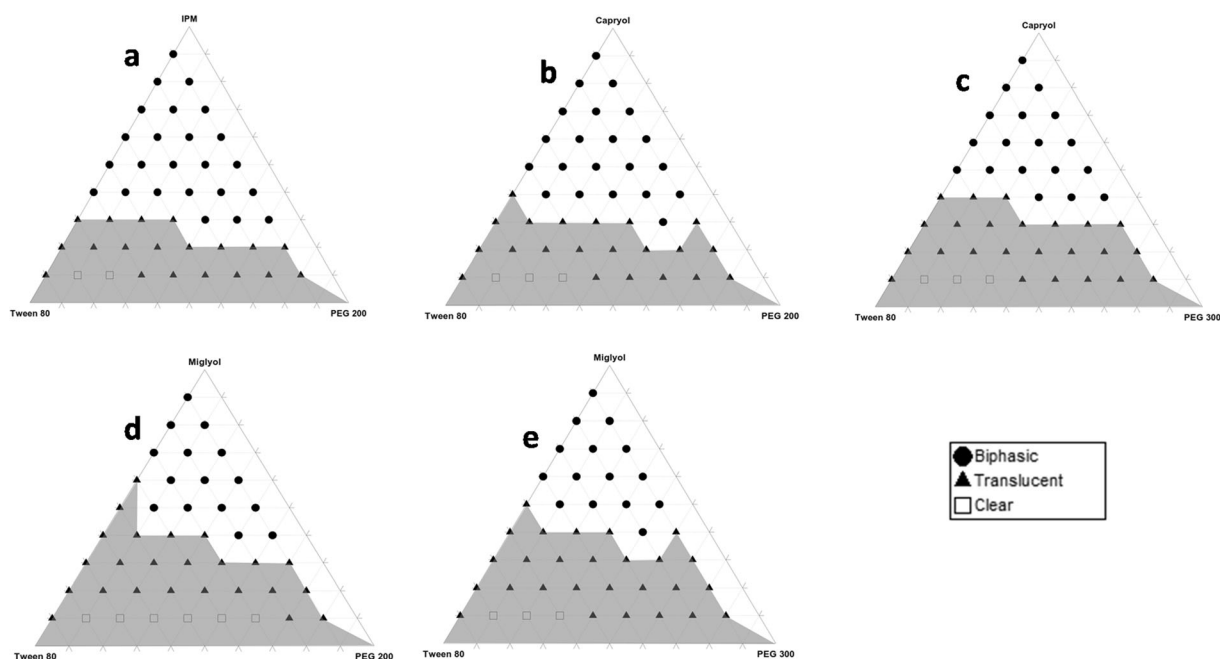


Fig. 1. Ternary phase diagram for (a) system I, (b) system III, (c) system IV, (d) system V and (e) system VI

Characterization of SNEGs

Differential Scanning Calorimetry

Differential scanning calorimetry (DSC) thermograms of formulae SNEG1, SNEG2, SNEG3, SNEG4, SNEG5, crude diacerein and Aeroperl are illustrated in Fig. 3.

The thermogram of diacerein exhibited an endothermic peak at 253.28°C, representing the melting point of the drug crystalline. The DSC thermogram of Aeroperl 300 showed broad endothermic peak at 75°C (25).

The characteristic peak of the drug disappeared in the formula thermogram.

Fourier Transform Infrared Spectroscopy

Diacerein spectrum exhibited one characteristic broad band at 3100–2600 cm^{-1} (OH stretching of carboxyl group). Two strong stretching bands for carbonyl groups appeared as at 1768 cm^{-1} (ester groups), and 1678 cm^{-1} (keto group merged with acid group) (5). The spectrum of Aeroperl 300

showed the same pattern of peaks as previously recorded by Khetarpal *et al.*, (26).

No significant differences were figured in the formula spectra, Fig. 4.

Powder X-Ray Diffraction

The patterns of XRD of SNEG3 (the optimized formula), diacerein and Aeroperl 300 are illustrated in Fig. 5. Diffractogram of the drug illustrated its crystalline nature and had sharp diffraction peaks at 5.25°, 10.49°, 17.45° and 27.9°, while the XRD pattern of Aeroperl 300 had no sharp peaks (25). The drug peaks disappeared in the pattern of XRD of the solid SNEG3.

Scanning Electron Microscopy

Scanning electron micrographs of the drug Aeroperl 300 and formula SNEG3 are illustrated in Fig. 6. Diacerein exhibited rod-shaped crystals while Aeroperl 300 appeared as spherical granules with a hollow interior. Figure 6c indicated complete disappearance of diacerein crystals in

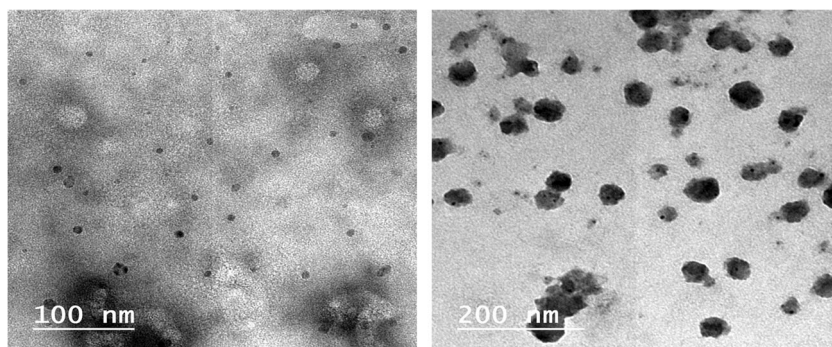


Fig. 2. TEM of the optimized formula F10 after dilution

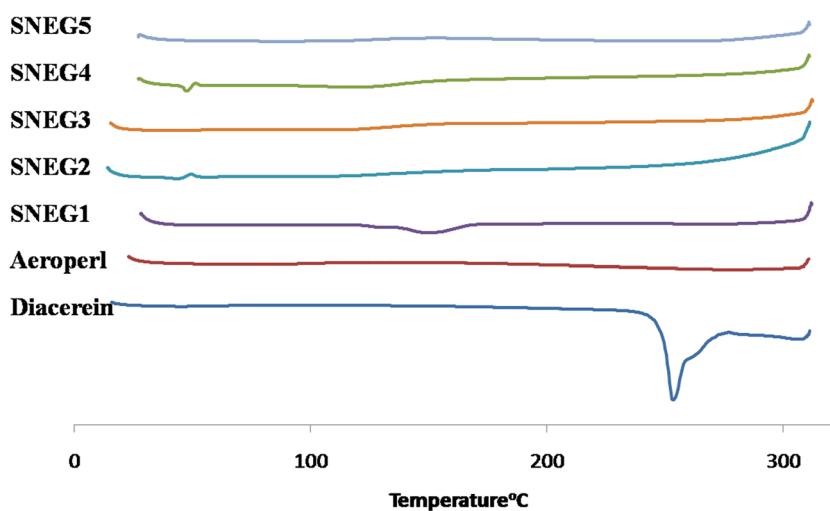


Fig. 3. DSC thermograms of diacerein, Aeroperl, SNEG1, SNEG2, SNEG3, SNEG4, and SNEG5

the scanning electron micrograph of formula SNEG3. Examination of the formula at a higher magnification power (Fig. 6d)

revealed that the smooth surface of Aeroperl 300 granules was covered with the nanoemulsion pre-concentrate.

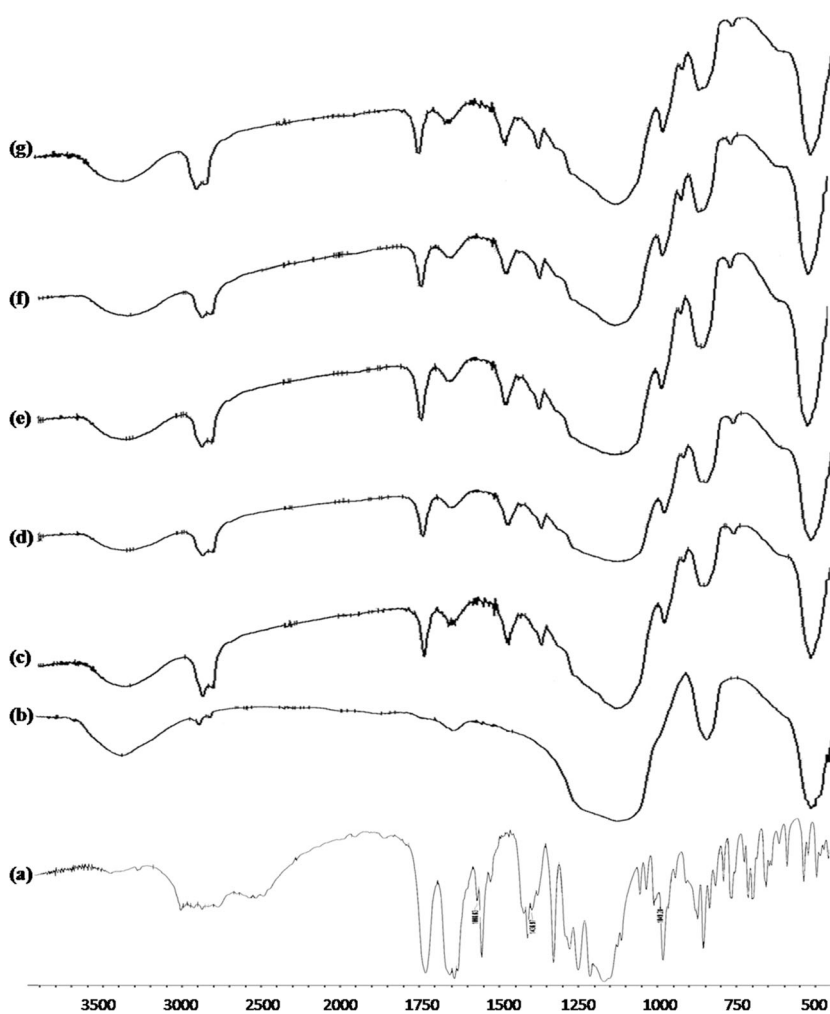


Fig. 4. FTIR patterns of (a) pure diacerein, (b) Aeroperl and (c) SNEG1, (d) SNEG2, (e) SNEG3, (f) SNEG4 and (g) SNEG5

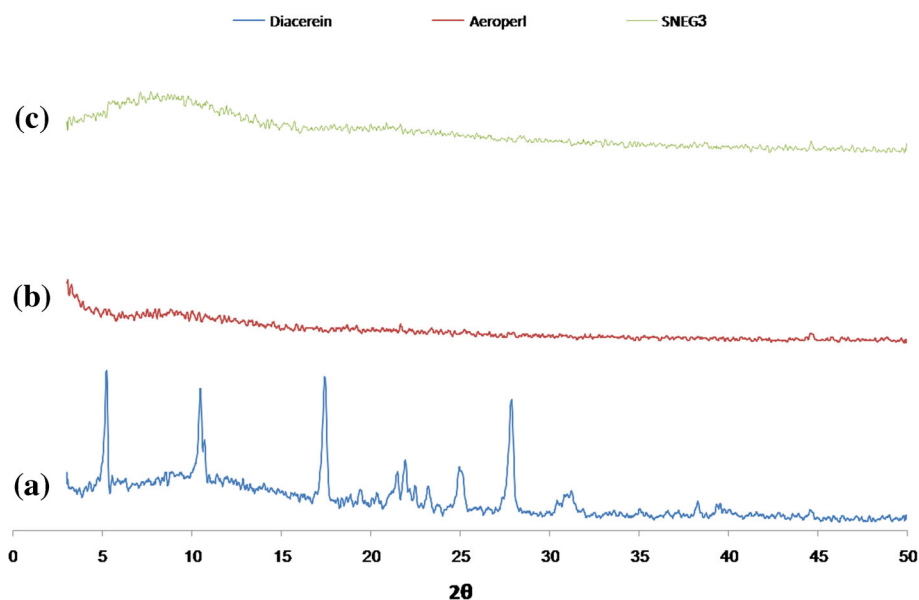


Fig. 5. X-ray diffractogram of (a) diacerein, (b) Aeroperl and (c) SNEG3

Carr's Index

The prepared formulae (SNEG1, SNEG4 and SNEG5) had Carr's index ranging from 30.01 ± 3.88 to $31.52 \pm 3.32\%$ which indicated poor flowability, while SNEG2 showed good flowability with Carr's index $14.84 \pm 1.19\%$ and SNEG3 exhibited passable flowability with Carr's index $23.32 \pm 3.88\%$ as shown in Table II (27).

Drug Content

Table II shows the mean values of diacerein content in different systems. Statistical *t* test results showed that there was

no significant difference at $p > 0.05$ between the actual mean drug content within all the formulae and the hypothetical value.

In Vitro Dissolution Study

Diacerein marketed product recorded the slowest dissolution rate, ($Q_5 = 2.14 \pm 0.12\%$) followed by diacerein powder with a dissolution rate, $15.15 \pm 7.28\%$. The prepared formulae (SNEG 1-5) significantly enhanced the dissolution rate, Q_5 values were more than 75%. All formulae showed higher $DE_{(0-30)}$, Q_5 and DR_5 and lower MDT than diacerein powder and the marketed product, Table II and Fig. 7.

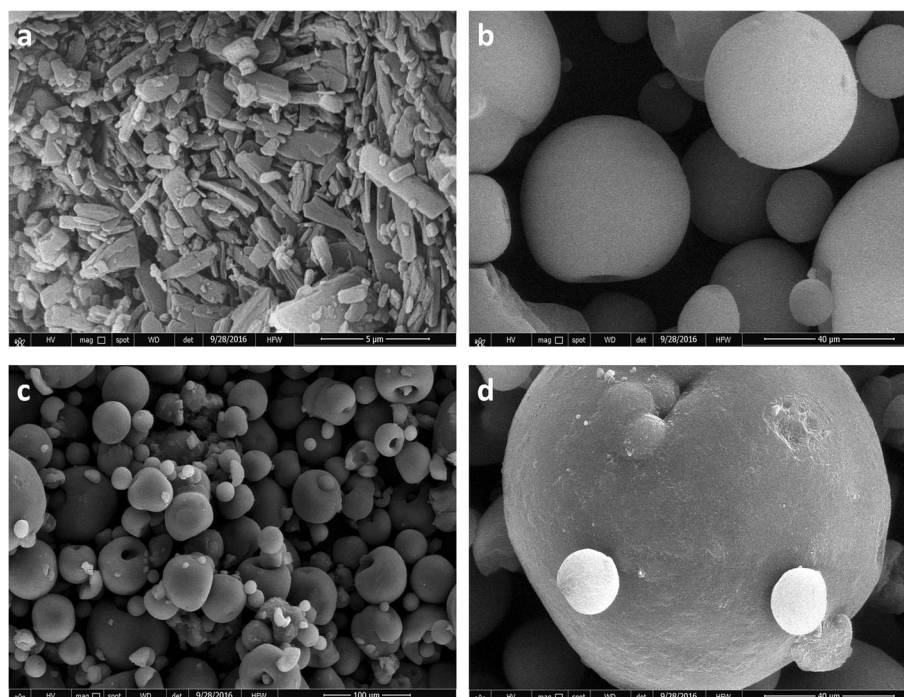


Fig. 6. Scanning electron micrographs of (a) diacerein, (b) Aeroperl and (c and d) formula SNEG3

Optimization of the Formulated SNEGs

The highest desirability value (0.795) was recorded for formula SNEG3 consisting of diacerein nanoemulsion preconcentrate with 10% Miglyol 812, 70% Tween 80 and 20% PEG 200 and adsorbed at 2:1 preconcentrate: Aeroperl. It recorded the highest Q_5 , D.E.(0–30), DR₅ and saturation solubility in water and the lowest MDT and Carr's index and was proposed for further evaluation.

In Vivo Evaluation

The liquid chromatography–mass spectrometry analysis of blank rabbit plasma mixed with hydrochlorothiazide and rhein illustrated that these peaks were isolated and eluted at 0.58 and 0.67 min, respectively. The assay technique exhibited that the relationship between the peak area ratio of rhein and its concentration was linear within the tested range and had a correlation of determination (r^2) of 0.999 and a mean extraction recovery of $98.95 \pm 3.829\%$.

The plasma concentration-time curves following administration of both SNEG3 and the diacerein capsule were illustrated in Fig. 8a. The mean values of C_{\max} for rhein were $6.29 \pm 0.607 \mu\text{g/mL}$ and $0.763 \pm 0.47 \mu\text{g/mL}$ following administration of SNEG3 and Diacerein capsule, respectively. The median t_{\max} was 0.167 and 0.333 h for the SNEG3 formula and the marketed product, respectively. In parallel with the C_{\max} , the mean $\text{AUC}_{0-\infty}$ values after oral administration of SNEG3 revealed greater values in comparison with the marketed diacerein capsules of $7.36 \pm 2.03 \mu\text{g.h/mL}$ and $2.44 \pm 0.61 \mu\text{g.h/mL}$, respectively, which resulted in a relative bioavailability of 377.42%. The elimination rate constant and half-life of rhein following the optimized SNEG3 formula were $0.2349 \pm 0.14 \text{ h}^{-1}$ and $4.036 \pm 2.88 \text{ h}$, whereas elimination rate constant and half-life of rhein following the administration of the marketed product was $0.1748 \pm 0.103 \text{ h}^{-1}$ and $5.734 \pm 4.63 \text{ h}$.

Two-way ANOVA exhibited that administration of SNEG3 recorded significantly higher C_{\max} and $\text{AUC}_{0-\infty}$

values than Diacerein capsule ($p < 0.05$). On the other hand, ANOVA test did not show any significant difference for rabbits effect. The statistical non-parametric test Wilcoxon signed rank for t_{\max} values showed a significant difference ($P < 0.05$) in the rate of drug absorption following oral administration of the marketed product and the investigated SNEG3 formula. ANOVA tests of half-life and elimination rate constant did not show any significant differences ($p > 0.05$) for formulae, and rabbits effect.

In Vitro/In Vivo Correlation

Figure 8b shows good IVIVCs for both SNEG3 and the marketed product when the percentage diacerein dissolved was plotted against the chosen AUCs. The correlation coefficient value for each line was very close to 1, where r^2 for SNEG3 IVIVC was 0.982 and r^2 for the marketed product IVIVC was 0.996.

DISCUSSION

All materials included for the preparation of SNEDDS were approved for oral use. Optimum drug loading could be achieved *via* proper choice of the surfactant, oil and co-surfactant for the drug under investigation. Oils were the main excipients because of their capability for solubilization of the lipophilic drug, and hence, the amount of the drug delivered through the intestinal lymphatic system would be improved, so the absorption from the GIT would be enhanced (28).

Capryol 90 is a saturated medium-chain-length oil (eight carbons) with hydrophilic–lipophilic balance (HLB) value = 6. Its amphiphilic nature enhances drug solubilization (29). Furthermore, Capryol 90 is known for its efficient self-emulsification capabilities that facilitate the formation of SNEDDS as reported by Nasr *et al.* (28).

The medium-chain triglyceride Miglyol 812 was selected as oily phase because of its good solubilization and fluidity

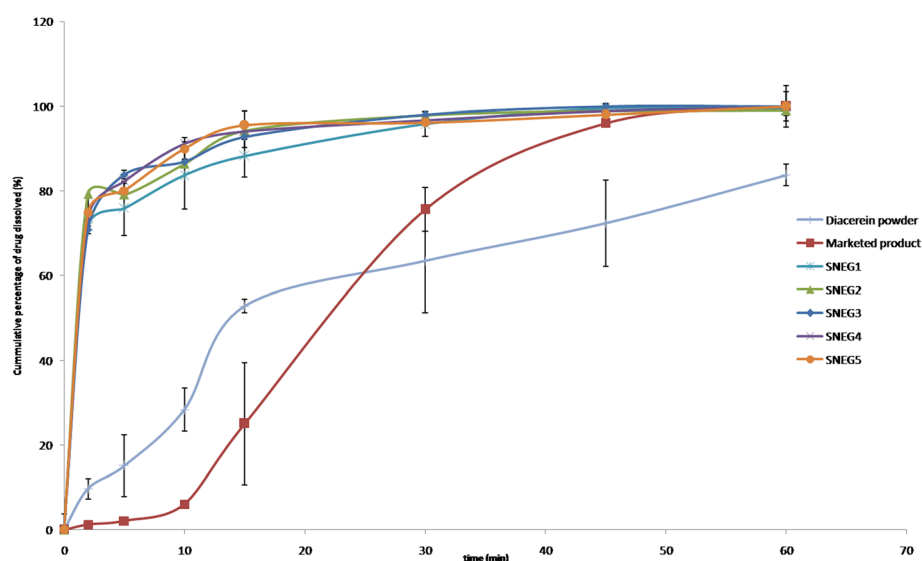


Fig. 7. *In vitro* dissolution profiles of diacerein from SNEG in comparison to the marketed product and diacerein powder in phosphate buffer pH 6.8

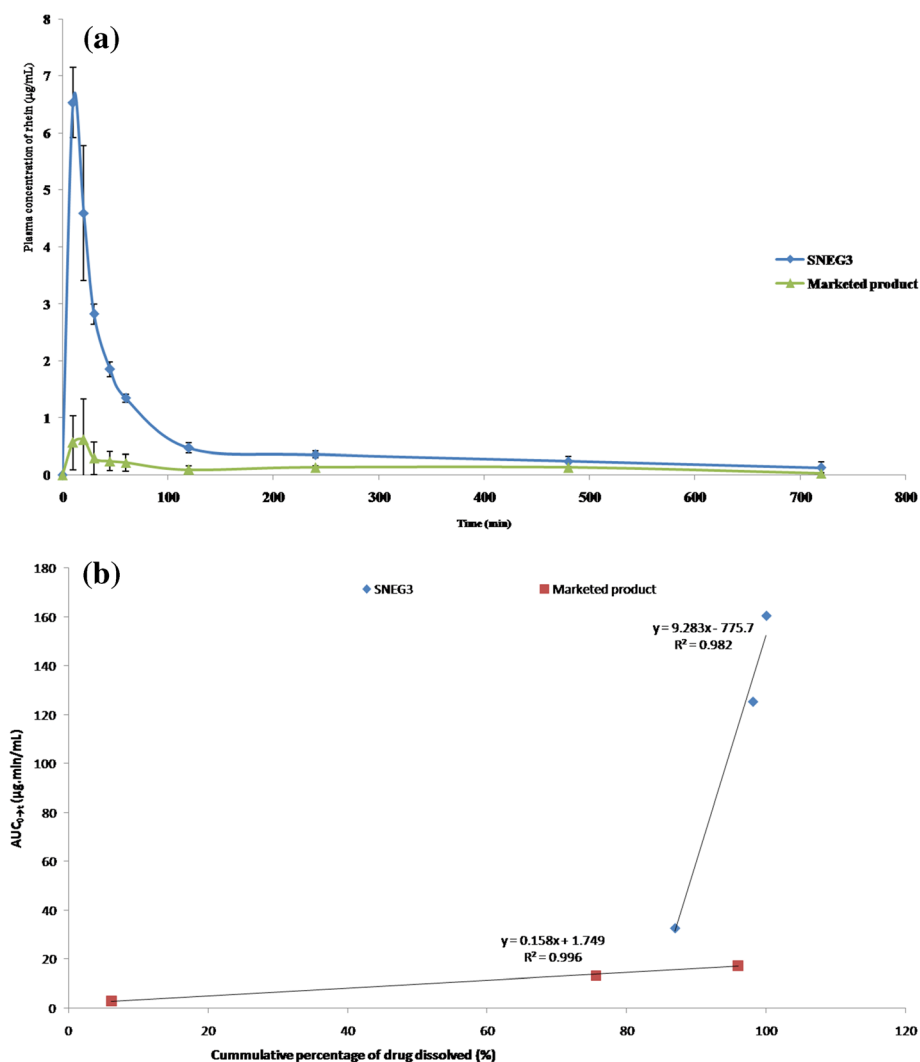


Fig. 8. (a) The mean plasma concentration time curve after the administration of the optimized SNEG formula and the marketed product and (b) Multiple level C IVIVC between $AUC_{0 \rightarrow t}$ for 10, 30 and 45 min and percentage of diacerein dissolved at these time points

characteristics and efficient self-emulsification capability. In addition, the complete saturation of Miglyol 812 prevents its oxidation with consequent enhanced chemical stability of drug substances. Furthermore, Miglyol 812 could be directly transported into the systemic circulation by the portal blood (30).

Moreover, it was reported by Nekkanti *et al.* (31) that medium-chain fatty acids (Capryol and Miglyol) could affect the tight junctions of the epithelial cells allowing paracellular transport.

Isopropyl myristate, a long-chain fatty acid, could improve drug bioavailability *via* stimulation of the lipoprotein synthesis and lymphatic absorption (31).

Being safe and biocompatible, nonionic surfactants had been preferred to ionic surfactants; hence, Tween 80 (HLB = 15) and Tween 20 (HLB = 16.7) were selected in our study (32,33). The efficiency of self-nanoemulsification was ascribed to the HLB value of the surfactant (34). Hydrophilic surfactants, with HLB values greater than 10, had the capability to form fine, uniform emulsion droplets that facilitated their rapid gastric emptying and offered a great surface area that led to enhanced

absorption. Furthermore, surfactants could provide a mechanical barrier to coalescence and prevent drug precipitation within the GI lumen *via* layer formation along the droplets of the emulsion that reduced the energy at the interface (28), as well as their inhibitory effects on P-glycoprotein and CYP450 enzymes could greatly augment their bioactivity as reported by Basalious *et al.* (14).

The components of the suggested 12 systems were mixed and investigated after high dilution with water to simulate the conditions which the nanoemulsion would face after administration.

Our results revealed that Miglyol and Capryol had larger nanoemulsion areas than IPM. This is similar to previous literature reported that the medium carbon chain length oils with higher HLB values as Miglyol (HLB 15.6) were superior to longer chain length oils with lower HLB values as IPM (35).

Results showed the use of oil with 10% concentration was optimum for nanoemulsion formation because destabilization of nanoemulsion caused by high dilution with water will not allow any higher concentrations of the oil to be solubilized (36).

Our findings revealed that only Tween 80 was more effective than Tween 20 in nanoemulsion formation. This was attributed to the dissimilarity in the molecular packing at the oil/water interface, so a greater proportion of the surfactant with short-chain fatty acid (Tween 20) was necessary for good emulsification (37).

The addition of a co-surfactant was necessary for nanoemulsion formation in the 12 systems for the fluidity of the interfacial film and appearance of transient negative interfacial tension. It could supply the interfacial film with the flexibility required for nanoemulsion formation *via* lowering the bending stress of the interface and this could be rarely achieved with the surfactant alone (28,38).

A good correlation could be seen between the appearance and the droplet sizes. As the concentration of Tween 80 increased, a clear nanoemulsion with smaller globule size and narrower size distribution was obtained. This reduction in MDS indicated the development of a better close-packed film of surfactants at oil/water interface, consequently stabilization of the oil droplets (30). Similarly, Radwan *et al.* and Gao (13,39), working on nanoemulsion, reported that increasing the surfactant ratio, decreased the globule size of nanoemulsion. This might be ascribed to condensation and stabilization of the interfacial film with the usage of surfactant; however, film expansion was obtained upon co-surfactant addition.

Based on our results, it was possible to obtain a stable and transparent nanoemulsion with droplet size below 50 nm when the S/CoS concentration was about 90% of SNEDDS formulation. This was in agreement with Nekkanti *et al.* (31).

The PDI is an indicator of homogeneity and size distribution of the examined system. It is a dimensionless number where PDI less than 0.5 reflected a homogenous distribution, while a greater than 0.5 indicated a higher heterogeneous dispersion (40).

The percentage transmittance is considered as a significant indicator for the isotropic nature of the formula. The 17 formulae showed % transmittance above 95% indicating optical clarity after dilution and ensuring that the droplet size of formulae in the nanometric range as the % transmittance is close to 100% (41).

A short self-emulsification time is a good indicator for rapid drug release in the GIT after oral administration. Kang *et al.* (42) reported that the good nanoemulsion preconcentrate can be solubilized in the medium using gentle mixing within 120 s.

Higher drug solubilities in Miglyol-based nanoemulsions could be ascribed to closeness of HLB value of Tween[®]80 (HLB = 15) to that of Miglyol[®]812 (HLB = 15.6) and consequently better emulsification and solubilization properties (43).

Formulae, namely F1, F9, F10, F11 and F15, were selected for adsorption to Aeroperl. The aforementioned formulae were chosen due to their low MDS ranging from 14.67 ± 1.07 to 24.1 ± 8.62 and low PDI in the range of 0.21–0.417, in addition to their high saturation solubility (higher than 5 mg/g).

The granules loaded with diacerein SNEDDS were investigated for physical interaction within formula using DSC. The thermogram of diacerein was in agreement with that reported by Aggarwal and Singh (5) who investigated the diacerein thermogram.

The disappearance of characteristic peak of the drug in the thermograms of the SNEG ensured the molecular dispersion of the drug through the formulae (29,42).

Regarding FTIR, no change was observed in the site and the trend of the diacerein absorption bands and the incorporation of diacerein into Aeroperl 300 did not change the sites and trends of peaks. Hence, there was no chemical interaction between Aeroperl 300 with diacerein. Moreover, the diminished intensities of the characteristic peaks of diacerein in SNEG could indicate the excipient dilution effect. The aforementioned results further provided the evidence for the absence of an interaction between diacerein and Aeroperl 300.

The disappearance of drug peaks in the pattern of XRD of the solid SNEG3 indicated the molecular dispersion of the drug within the nanoemulsion formula. The amorphous dispersion of diacerein within the solid SNEG afforded additional explanation for the improvement in drug solubility. This coincided with previous results recorded by Shanmugam *et al.* (44).

The structure of Aeroperl 300 under SEM might increase its surface area, and improve its adsorption capacity, so Aeroperl could be considered as a powerful adsorbent. Complete disappearance of diacerein crystals in the scanning electron micrograph of formula SNEG3 provided strong proof that the drug had been completely molecularly dispersed within the solid nanoemulsion and ensured absence of precipitation or crystallization of the drug within the formula. Examination of the formula at a higher magnification ensured the efficiency of the method used for preparation of SNEG.

The improved drug dissolution by SNEG formulated using porous carriers could be ascribed to the rapid desorption of the liquid SNEDDS from silica surface with spontaneous nanoemulsion formation of the lipophilic drug upon contact to the dissolution medium due to the stronger physical interactions between silica and phosphate buffer compared to silica and liquid SNEDDS. This was only noticed by Planinšek *et al.* (45) in his work on carvedilol dissolution. Furthermore, the great surface area of these particles led to enhanced dissolution compared to pure diacerein. The improved wetting of dispersion granules might be considered an additional parameter that affected dissolution rate of SNEG owing to enhanced penetration of dissolution medium into the voids and capillaries of these granules. Diffusion and convection of liquid SNEDDS when porous carriers exposed to dissolution medium might control the drug release from SNEG (46).

The *in vivo* study results revealed higher C_{max} and $AUC_{0-\infty}$ with lowered t_{max} of the optimized formula compared to the marketed product indicating the enhanced extent and rate of drug absorption. SNEG3 produced a 3.77-fold increase in bioavailability, as compared to diacerein capsule. So, the dose of SNEG could be reduced to one quarter of the total dose to achieve the same bioavailability of the marketed product and this might reduce the unabsorbed part of rhein in the colon decreasing the adverse effects due to the drug. In addition to that, the recorded C_{max} (6.29 $\mu\text{g/mL}$) of rhein in plasma was comparable to El-Laithy *et al.* study (2), where the reported C_{max} of rhein ranged from (6.92 to 16.9 $\mu\text{g/mL}$).

The successful IVIVCs confirmed that the *in vitro* dissolution study condition and result was representative to the *in vivo* pharmacokinetic study. So, the *in vivo* bioavailability may be

bioavailed and the *in vitro* dissolution test could be used as an alternative.

The main approach for enhancing the bioavailability of diacerein was ascribed to the capability of SNEG3 to solubilize the hydrophobic drug in the nanoemulsion droplets leading to the enhancement of the portal blood absorption of diacerein. Furthermore, using medium-chain fatty acid (Miglyol) might affect the tight junctions of the epithelial cells, hence allowing paracellular transport (31). The optimized SNEG3 showed marked increase of diacerein solubility and rapid dissolution rate as well as improved portal absorption, and this led to minimized side effects caused by the unabsorbed part of rheim in the colon. It was worthy to say that the enhanced bioavailability of diacerein achieved via SNEG3 could allow the use of lower doses of diacerein, thus minimizing its side effects during treatment of osteoarthritis.

CONCLUSION

The enhanced bioavailability of diacerein achieved via the optimized formula could allow the use of lower doses of diacerein, thus minimizing its side effects caused by the unabsorbed part of rheim in the colon during treatment of osteoarthritis. Clinical evaluation on human volunteers is suggested to be assessed in the future for dose correction.

COMPLIANCE WITH ETHICAL STANDARDS

The experiment protocol was accepted by the Research Ethics Committee of Faculty of Pharmacy, Cairo University, Cairo, Egypt (PI 911).

Conflict of Interest The authors declare that there is no conflict of interest.

REFERENCES

- Elsayed I, Abdelbary AA, Elshafeey AH. Nanosizing of a poorly soluble drug: technique optimization, factorial analysis, and pharmacokinetic study in healthy human volunteers. *Int J Nanomedicine*. 2014;9:2943.
- El-Laithy HM, Basalious EB, El-Hoseiny BM, Adel MM. Novel self-nanoemulsifying self-nanosuspension (SNESNS) for enhancing oral bioavailability of diacerein: simultaneous portal blood absorption and lymphatic delivery. *Int J Pharm*. 2015;490(1):146–54.
- Maski N, Kumaran A, Girhepunje K, Ghode P, Randive S, Pal R. Studies on the preparation, characterization and solubility of β -cyclodextrin-diacerein inclusion complexes. *Int J Pharm Pharm Sci*. 2009;1(2):121–35.
- Jain A, Singh SK, Singh Y, Singh S. Development of lipid nanoparticles of diacerein, an antiosteoarthritic drug for enhancement in bioavailability and reduction in its side effects. *J Biomed Nanotechnol*. 2013;9(5):891–900.
- Aggarwal AK, Singh S. Physicochemical characterization and dissolution study of solid dispersions of diacerein with polyethylene glycol 6000. *Drug Dev Ind Pharm*. 2011;37(10):1181–91.
- Abdelbary AA, Elshafeey AH, El-Nabarawi M, Ellassasy A, Li X, Jasti B. Comparative *in vivo* evaluation of aripiprazole coprecipitate, nanoparticles and marketed tablets in healthy human volunteers and *in vitro-in vivo* correlation. *Curr Trends Biotechnol Pharm*. 2011;5(4):1397–409.
- Xi J, Chang Q, Chan CK, Meng ZY, Wang GN, Sun JB, et al. Formulation development and bioavailability evaluation of a self-nanoemulsified drug delivery system of oleanolic acid. *AAPS PharmSciTech*. 2009;10(1):172–82.
- Date AA, Desai N, Dixit R, Nagarsenker M. Self-nanoemulsifying drug delivery systems: formulation insights, applications and advances. *Nanomedicine*. 2010;5(10):1595–616.
- Kassem AA, Mohsen AM, Ahmed RS, Essam TM. Self-nanoemulsifying drug delivery system (SNEDDS) with enhanced solubilization of nystatin for treatment of oral candidiasis: design, optimization, *in vitro* and *in vivo* evaluation. *J Mol Liq*. 2016;218:219–32.
- Tang B, Cheng G, Gu J-C, Xu C-H. Development of solid self-emulsifying drug delivery systems: preparation techniques and dosage forms. *Drug Discov Today*. 2008;13(13):606–12.
- Soliman KA, Ibrahim HK, Ghorab MM. Formulation of avanafil in a solid self-nanoemulsifying drug delivery system for enhanced oral delivery. *Eur J Pharm Sci*. 2016;93:447–55.
- El Maghraby GM. Transdermal delivery of hydrocortisone from eucalyptus oil microemulsion: effects of cosurfactants. *Int J Pharm*. 2008;355(1):285–92.
- Radwan SAA, ElMeshad AN, Shoukri RA. Microemulsion loaded hydrogel as a promising vehicle for dermal delivery of the antifungal sertaconazole: design, optimization and *ex vivo* evaluation. *Drug Dev Ind Pharm*. 2017;43(8):1351–65.
- Basalious EB, Shawky N, Badr-Eldin SM. SNEDDS containing bioenhancers for improvement of dissolution and oral absorption of lacidipine. I: development and optimization. *Int J Pharm*. 2010;391(1):203–11.
- Xue X, Cao M, Ren L, Qian Y, Chen G. Preparation and optimization of rivaroxaban by self-nanoemulsifying drug delivery system (SNEDDS) for enhanced oral bioavailability and no food effect. *AAPS PharmSciTech*. 2018;19(4):1847–59.
- Jain A, Kaur R, Beg S, Kushwah V, Jain S, Singh B. Novel cationic supersaturable nanomicellar systems of raloxifene hydrochloride with enhanced biopharmaceutical attributes. *Drug Deliv Transl Res*. 2018;1–23.
- Badawi AA, El-Laithy HM, El Qidra RK, El Mofty H. Chitosan based nanocarriers for indomethacin ocular delivery. *Arch Pharm Res*. 2008;31(8):1040–9.
- Patil SB, Shete DK, Narade SB, Surve SS, Khan ZK, Bhise SB, et al. Improvement in the dissolution profile of diacerein using a surfactant-based solid dispersion technique. *Drug Discov Ther*. 2010;4(6):435–41.
- Khan K. The concept of dissolution efficiency. *J Pharm Pharmacol*. 1975;27(1):48–9.
- Ibrahim HK, Fahmy RH. Localized rosuvastatin via implantable bioerodible sponge and its potential role in augmenting bone healing and regeneration. *Drug Deliv*. 2016;23(9):3181–92.
- Derringer G, Suich R. Simultaneous optimization of several response variables. *J Qual Technol*. 1980;12(4):214–9.
- Pathak A, Rajput SJ. Diacerein nanosuspension: process optimization, physicochemical characterization, cytotoxicity assessment and *in-vivo* evaluation for oral bioavailability enhancement. *Pharm Res*. 2016;6(10):6595–615.
- Volpato NM, Silva RL, Brito APP, Gonçalves JCS, Vaisman M, Noël F. Multiple level C *in vitro/in vivo* correlation of dissolution profiles of two l-thyroxine tablets with pharmacokinetics data obtained from patients treated for hypothyroidism. *Eur J Pharm Sci*. 2004;21(5):655–60.
- Aziz DE, Abdelbary AA, Ellassasy AI. Fabrication of novel elastosomes for boosting the transdermal delivery of diacerein: statistical optimization, *ex-vivo* permeation, *in-vivo* skin deposition and pharmacokinetic assessment compared to oral formulation. *Drug Deliv*. 2018;25(1):815–26.
- Shrivastava AR, Ursekar B, Kapadia CJ. Design, optimization, preparation and evaluation of dispersion granules of valsartan and formulation into tablets. *Curr Drug Deliv*. 2009;6(1):28–37.
- Khetarpal NA, Ramachal AKS, Rao L, Amin PD. Formulation development of a stable solid oral dosage form of Valproic acid using colloidal silica. *Int J Drug Deliv*. 2012;4(2):266.
- Sandhya S, Gowthami G, Vinod K, VidyaSraavanthi E, Saikumar P, Rao K. Formulation and evaluation of herbal effervescent granules incorporated with *Limnophila indica* extract for bacillary dysentery. *Ann Bio Res*. 2012;3(1):63–72.

28. Nasr A, Gardouh A, Ghorab M. Novel solid self-nanoemulsifying drug delivery system (S-SNEDDS) for oral delivery of olmesartan medoxomil: design, formulation, pharmacokinetic and bioavailability evaluation. *Pharmaceutics*. 2016;8(3):20.
29. Balakrishnan P, Lee B-J, Oh DH, Kim JO, Hong MJ, Jee J-P, et al. Enhanced oral bioavailability of dexibuprofen by a novel solid self-emulsifying drug delivery system (SEDDS). *Eur J Pharm Biopharm*. 2009;72(3):539–45.
30. El-Laithy HM. Self-nanoemulsifying drug delivery system for enhanced bioavailability and improved hepatoprotective activity of biphenyl dimethyl dicarboxylate. *Curr Drug Deliv*. 2008;5(3):170–6.
31. Nekkanti V, Karatgi P, Prabhu R, Pillai R. Solid self-microemulsifying formulation for candesartan cilexetil. *AAPS PharmSciTech*. 2010;11(1):9–17.
32. Zhao Y, Wang C, Chow AH, Ren K, Gong T, Zhang Z, et al. Self-nanoemulsifying drug delivery system (SNEDDS) for oral delivery of Zedoary essential oil: formulation and bioavailability studies. *Int J Pharm*. 2010;383(1):170–7.
33. Constantinides PP, Scalart J-P, Lancaster C, Marcello J, Marks G, Ellens H, et al. Formulation and intestinal absorption enhancement evaluation of water-in-oil microemulsions incorporating medium-chain glycerides. *Pharm Res*. 1994;11(10):1385–90.
34. Singh AK, Chaurasiya A, Awasthi A, Mishra G, Asati D, Khar RK, et al. Oral bioavailability enhancement of exemestane from self-microemulsifying drug delivery system (SMEDDS). *AAPS PharmSciTech*. 2009;10(3):906–16.
35. Elnaggar YS, El-Massik MA, Abdallah OY. Self-nanoemulsifying drug delivery systems of tamoxifen citrate: design and optimization. *Int J Pharm*. 2009;380(1):133–41.
36. Morey TE, Modell JH, Shekhawat D, Grand T, Shah DO, Gravenstein N, et al. Preparation and anesthetic properties of propofol microemulsions in rats. *J Am Soc Anesthesiol*. 2006;104(6):1184–90.
37. Attwood D, Mallon C, Ktistis G, Taylor C. A study on factors influencing the droplet size in nonionic oil-in-water microemulsions. *Int J Pharm*. 1992;88(1):417–22.
38. Kawakami K, Yoshikawa T, Moroto Y, Kanaoka E, Takahashi K, Nishihara Y, et al. Microemulsion formulation for enhanced absorption of poorly soluble drugs: I. Prescription design. *J Control Release*. 2002;81(1):65–74.
39. Gao Z-G. Thermal reversible microemulsion for oral delivery of poorly water-soluble drugs. In: *Thermal reversible microemulsion for oral delivery of poorly water-soluble drugs*: INTECH open access publisher; 2012.
40. Chavda H, Patel J, Chavada G, Dave S, Patel A, Patel C. Self-nanoemulsifying powder of isotretinoin: preparation and characterization. *J Powder Technol*. 2013;2013:1–9.
41. Khan AW, Kotta S, Ansari SH, Sharma RK, Ali J. Self-nanoemulsifying drug delivery system (SNEDDS) of the poorly water-soluble grapefruit flavonoid Naringenin: design, characterization, in vitro and in vivo evaluation. *Drug Deliv*. 2015;22(4):552–61.
42. Kang JH, Oh DH, Oh Y-K, Yong CS, Choi H-G. Effects of solid carriers on the crystalline properties, dissolution and bioavailability of flurbiprofen in solid self-nanoemulsifying drug delivery system (solid SNEDDS). *Eur J Pharm Biopharm*. 2012;80(2):289–97.
43. Vander Kloet J, Schramm LL, Shelfantook B. Application of the hydrophile-lipophile balance concept to the classification of demulsifiers and bituminous froth and its components. *Fuel Process Technol*. 2002;75(1):9–26.
44. Shanmugam S, Baskaran R, Balakrishnan P, Thapa P, Yong CS, Yoo BK. Solid self-nanoemulsifying drug delivery system (S-SNEDDS) containing phosphatidylcholine for enhanced bioavailability of highly lipophilic bioactive carotenoid lutein. *Eur J Pharm Biopharm*. 2011;79(2):250–7.
45. Planinšek O, Kovačič B, Vrečer F. Carvedilol dissolution improvement by preparation of solid dispersions with porous silica. *Int J Pharm*. 2011;406(1):41–8.
46. Beg S, Swain S, Singh HP, Patra CN, Rao MB. Development, optimization, and characterization of solid self-nanoemulsifying drug delivery systems of valsartan using porous carriers. *AAPS PharmSciTech*. 2012;13(4):1416–27.